

Observation of a Dipolar Quantum Gas with Metastable Supersolid Properties

L. Tanzi,^{1,2} E. Lucioni,^{1,2} F. Famà,¹ J. Catani,^{2,3} A. Fioretti,¹ C. Gabbanini,¹
R. N. Bisset,⁴ L. Santos,⁴ and G. Modugno^{1,2,*}

¹CNR-INO, Sede Secondaria "Adriano Gozzini," via Moruzzi 1, 56124 Pisa, Italy

²LENS and Dipartimento di Fisica e Astronomia, Università di Firenze, 50019 Sesto Fiorentino, Italy

³CNR-INO, Sede Secondaria Sesto Fiorentino, 50019 Sesto Fiorentino, Italy

⁴Institut für Theoretische Physik, Leibniz Universität Hannover, Appelstrasse 2, 30167 Hannover, Germany



(Received 6 November 2018; published 3 April 2019)

The competition of dipole-dipole and contact interactions leads to exciting new physics in dipolar gases, well illustrated by the recent observation of quantum droplets and rotons in dipolar condensates. We show that the combination of the roton instability and quantum stabilization leads under proper conditions to a novel regime that presents supersolid properties due to the coexistence of stripe modulation and phase coherence. In a combined experimental and theoretical analysis, we determine the parameter regime for the formation of coherent stripes, whose lifetime of a few tens of milliseconds is limited by the eventual destruction of the stripe pattern due to three-body losses. Our results open intriguing prospects for the development of long-lived dipolar supersolids.

DOI: [10.1103/PhysRevLett.122.130405](https://doi.org/10.1103/PhysRevLett.122.130405)

Superfluidity and crystalline order are seemingly mutually exclusive properties. However, rather counterintuitively, both properties may coexist, resulting in an intriguing new phase known as the supersolid phase [1–4]. Although proposed 50 years ago in ⁴He research, its experimental realization remains to this date elusive [5]. Recently, the idea of supersolidity has been revisited in the context of ultracold atoms. The coexistence of phase coherence and density modulation has been reported in Bose-Einstein condensates (BECs) in optical cavities [6] and in the presence of synthetic spin-orbit coupling [7]. The modulation in these systems is, however, infinitely stiff since it is externally imposed.

This stiffness may be overcome in dipolar gases [8,9], allowing the realization of supersolids genuinely resulting from interparticle interactions. Two recent experimental developments open exciting perspectives in this direction. On the one hand, the interplay of anisotropic dipole-dipole interactions, isotropic contact interactions, and external confinement may lead to the appearance of a dispersion minimum that resembles the celebrated helium roton [10]. Dipolar rotons have been observed very recently in experiments with erbium atoms [11,12]. Interestingly, by decreasing the *s*-wave scattering length, the roton gap may be easily reduced until it vanishes, resulting in the so-called roton instability [10]. Although in the absence of stabilizing forces such an instability results in local collapses [13], a repulsive force at short range could stabilize a supersolid [14–16]. Interestingly, such a stabilization mechanism may be provided by quantum fluctuations [17], whose role is dramatically enhanced by the competition of dipole-dipole and contact interactions [18–21]. Quantum stabilization

results in the formation of stable quantum droplets, as recently observed in a series of remarkable experiments [22–25], also demonstrating their self-bound nature [25]. In the presence of a trap, regular arrays of multiple droplets form due to dipolar repulsion [22,23,26]. They, however, lack the necessary coherence to establish a supersolid phase due to the weak tunneling between neighboring droplets [26,27]. Very recently, it has been predicted that stationary states of a dipolar Bose gas may acquire supersolid characteristics under the appropriate conditions [27,28].

In this Letter, we show that ramping through the rotonic instability [11] in a weakly confined, strongly dipolar dysprosium BEC results in the formation of a metastable, coherent stripe modulation, in a narrow range of scattering lengths close to the instability. By means of a combined experimental and theoretical investigation, we study the dynamics of the emerging density modulation, identifying the novel coherent regime as an array of weakly bound droplets with a significant overlap and well-defined phase relation. Hence the stripes present supersolid properties, although they have a finite lifetime due to three-body losses. The stripe regime has distinct properties from the incoherent regime appearing for lower scattering length, which we identify as arrays of strongly bound, but rapidly decaying droplets [23,26]. Our results open exciting perspectives for the realization of long-lived dipolar supersolids.

Our experiment is based on a BEC of ¹⁶²Dy atoms, with typical atom number $N = 4 \times 10^4$ and undetectable thermal component [29,30]. Two crossed optical potentials create a trap with frequencies $\omega_{x,y,z} = 2\pi(18.5, 53, 81)$ Hz. A homogeneous magnetic field *B* aligns the dipoles along

the z axis. Dy atoms in their ground state have a dipolar length $a_{dd} = \mu_0 \mu^2 m / 12 \pi \hbar^2 \simeq 130 a_0$, for mass m and dipole moment μ . The s -wave scattering length a_s is controlled via a magnetic Feshbach resonance located around 5.1 G [31,32]. The condensate is initially created with a_s close to the background value $a_{bg} = 157(4) a_0$ [31]. The magnetic field is then changed slowly in time to decrease a_s , with a final ramp from a stable BEC at $a_s = 108 a_0$ into the roton instability [32].

Our observable is the density distribution after 62 ms of free expansion at the final a_s , detected by absorption imaging along the z direction. We interpret it as the momentum distribution $n(k_x, k_y)$ in the (x, y) plane [32]. As a function of the final a_s , we observe three distinct regimes. For large a_s , the condensate does not qualitatively change compared to the initial BEC (the BEC regime). At intermediate a_s , the BEC develops a striplike modulation, but global phase coherence is preserved (the stripe regime). Finally for low a_s , global phase coherence and stripe regularity are rapidly lost (incoherent regime). In the following, we characterize in detail these regimes.

Figure 1(a) shows time-of-flight pictures for three different final a_s at different hold times t after the end of the ramp. The upper panel, for $a_s \simeq 108 a_0$, illustrates the BEC regime. As the scattering length is lowered to $a_s \simeq 94 a_0$, for a limited range of scattering lengths, a stripe modulation spontaneously emerges (middle panel): the momentum distribution shows small side peaks along the weak trap axis, with characteristic momentum $\bar{k}_x = 1.2(2) \mu\text{m}^{-1}$, close to the roton momentum predicted for an unconfined system at the instability, $k_{\text{rot}} = 1.53 \mu\text{m}^{-1}$ [11,32]. The shape of $n(k_x, k_y)$ is reproducible from shot to shot and is maintained for several tens of milliseconds. For longer times ($t \gtrsim 100$ ms), an unmodulated BEC is recovered. For smaller a_s values (bottom panel), $n(k_x, k_y)$ presents structures also along k_y , with maxima and minima distributed irregularly in the (k_x, k_y) plane, as well as very large shot-to-shot variations. At longer times, we observe small condensates with large thermal fractions.

There is a marked dependence on N of the critical scattering length at which we observe the onset of the modulated regimes. Figure 1(b) shows the evolution of a phenomenological observable that quantifies the deviation of the momentum distribution from that of a BEC. One notes a region of small deviations for large a_s (BEC regime), clearly separated from a region of large deviations for smaller a_s . The trend of the critical a_s is reasonably well reproduced by numerical calculations based on the theory of roton instability [11,32].

The time evolution of the atom number $N(t)$ is shown in Fig. 2(a). Both stripe and incoherent regimes feature an initial loss on timescales much faster than the typical lifetime of a BEC at $B = 5.305$ G, $\tau_{\text{BEC}} \simeq 500$ ms [32]. We can estimate the *in situ* mean density from the loss rate

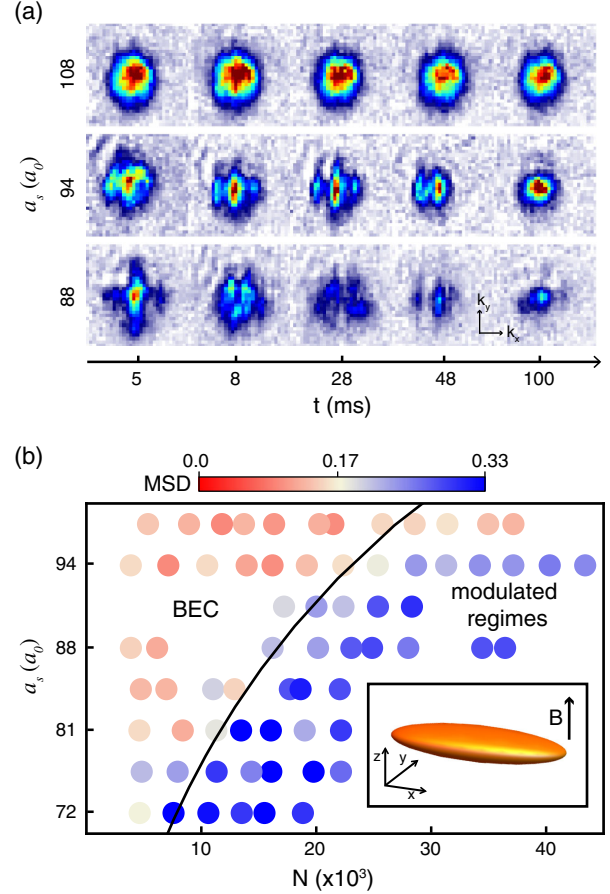


FIG. 1. (a) Typical momentum distribution $n(k_x, k_y)$ for different evolution times in three regimes: (top row) $B = 5.305$ G ($a \simeq 108 a_0$, BEC regime); (middle row) $B = 5.279$ G ($a \simeq 94 a_0$, stripe regime); (bottom row) $B = 5.272$ G ($a \simeq 88 a_0$, incoherent regime). (b) Mean squared deviation (MSD) of $n(k_x, k_y)$ from a Gaussian, distinguishing BEC and stripe or incoherent regions in the B - N plane [32]. The black line represents the theoretical prediction for the roton instability [11,32]. (Inset) Trap geometry.

since $\dot{N}/N = -L_3 \langle n^2 \rangle$, with $\langle n^2 \rangle$ being the mean quadratic density. Using the recombination constant measured from the decay of the stable BEC at $B = 5.305$ G, $L_3 = 2.5(3) \times 10^{-28} \text{ cm}^6 \text{ s}^{-1}$, we estimate a similar mean density of order $n \simeq 5 \times 10^{14} \text{ cm}^{-3}$, for both stripe and incoherent regimes [32]. This is about 10 times larger than the calculated BEC density, suggesting that, in both modulated regimes, the Lee-Huang-Yang (LHY) repulsion has a stabilizing role [17–21,23].

We analyze the stripe regime by fitting the y -averaged distributions $n(k_x)$ with a two-slit model $n(k_x) = C_0 \exp(-k_x^2/2\sigma_x^2)[1 + C_1 \cos^2(\pi k_x/\bar{k}_x + \phi)]$. The interference amplitude A is defined as the relative weight of the side peaks in $n(k_x)$ with respect to the central one [32], and it provides information on the depth of the density modulation. The interference phase ϕ provides instead a measure of the robustness of the stripe pattern, both in what

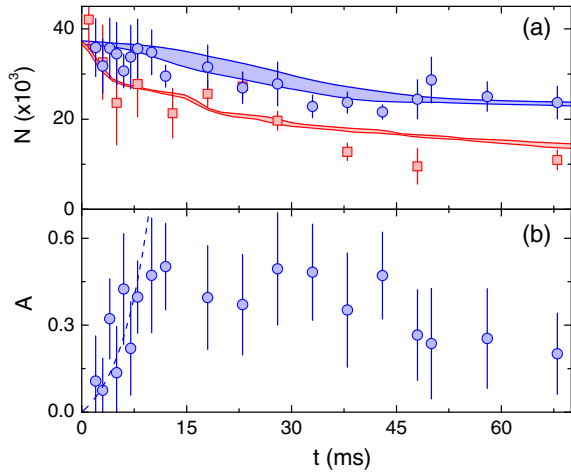


FIG. 2. (a) Time evolution of the atom number for stripes ($B = 5.279$ G, blue circles) and incoherent ($B = 5.272$ G, red squares) regimes. Blue and red shaded areas represent the atom loss predicted by our dynamical simulations at $a_s \simeq 94a_0$ and $a_s \simeq 88a_0$, respectively. (b) Time evolution of the interference amplitude A in the stripe regime ($B = 5.279$ G). The dashed line is an exponential fit to the initial ($t \leq 10$ ms) growth. The error bars represent the standard deviation of about 40 measurements.

concerns the phase locking between the stripes and their relative distances.

Figure 2(b) shows the evolution of A in the stripe regime. The initial exponential growth is consistent with the onset of the roton instability observed in previous experiments [11]. After this initial growth, A remains approximately constant for about 30 ms and then decreases. The reduction of A at longer times gives evidence of the progressive disappearance of the stripe modulation, compatible with the reduction of the atom loss rate observed in Fig. 2(a).

Figure 3 shows the key observations for the coherence. Figure 3(a) depicts the time evolution of the variance $\Delta\phi^2$ in the stripe regime, obtained from about 40 realizations for each evolution time. At the initial stages of the rotonic instability, we observe a large variation of ϕ , which may be explained due to shot-to-shot differences in the quantum and thermal seeding of the instability that lead to a marked variation, for a fixed time, of A . Remarkably, we observe that after the stripe formation (the first 10 ms), $\Delta\phi^2$ remains small for approximately 20 ms, revealing that the stripes remain stable and coherent for a time significantly longer than their formation time. After this time, $\Delta\phi^2$ increases, eventually reaching the expectation value for a uniformly distributed ϕ , corresponding to a fully incoherent or disorganized stripe pattern.

When decreasing the final a_s , the system enters the incoherent regime. In order to compare stripe and incoherent regimes, we study their average momentum distribution over approximately 40 absorption images at different evolution times; see Fig. 3(b). The persisting side peaks in the stripe regime confirm the existence of a stable

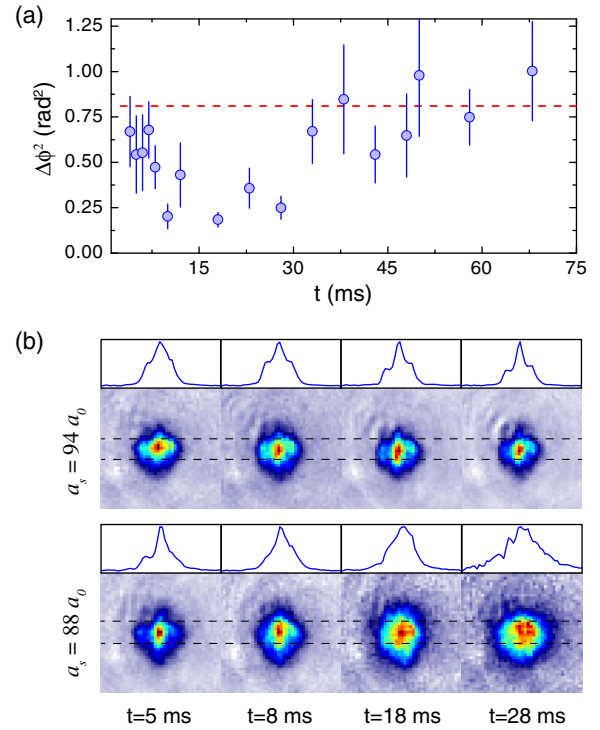


FIG. 3. (a) Time evolution of the interference phase variance $\Delta\phi^2$ in the stripe regime ($a_s \simeq 94a_0$). The error bars correspond to $\Delta\phi^2/2/(N-2)$, with $N \simeq 40$ being the number of measurements for each dataset. The red-dashed line is the expected variance for a uniformly distributed phase. (b) Averaged momentum distribution $\bar{n}(k_x, k_y)$ over 40 absorption images (top panel) in the stripe regime and (bottom panel) in the incoherent regime at different evolution times. The profiles are obtained by integrating $\bar{n}(k_x, k_y)$ along k_y in the region between dashed lines.

coherent stripe pattern. In contrast, when a_s is reduced into the incoherent regime, side peaks are visible only during the pattern formation ($t = 5$ ms), whereas already at $t = 18$ ms no clear pattern is recognizable, showing that coherence and/or pattern stability is quickly lost after the instability develops.

In direct support of our experiments, we have performed realistic 3D simulations of the dynamics during and after the ramp of a_s using the generalized Gross-Pitaevskii equation, which includes the stabilizing effects of quantum fluctuations [18,21,23,24]. We also seed the initial states with quantum and thermal fluctuations according to the truncated-Wigner prescription, include three-body losses, and the $a_s(B)$ dependence that, within the experimental uncertainty, provides the best experiment-theory agreement [32]. The simulations support the experimental observations and provide key insights into the nature of both stripe and incoherent regimes. First of all, they confirm that the observed stripe regime is triggered by a roton instability, similar to the one observed in an Er system [11], but in our experiments the instability leads to a long-lived density modulation due to the stabilizing role of quantum

fluctuations. This is shown, for example, by the good agreement of theory and experiment for $N(t)$ in both the stripe and incoherent regime [see Fig. 2(a)], which confirms that the atom number decay is due to the appearance of high-density modulations, where the LHY energy plays a significant role.

The most important results of the simulations are summarized in Fig. 4. They confirm a marked difference between the observed stripe and incoherent regimes. Since simulating the dynamics during the free expansion is challenging [11], we study the in-trap density and phase distributions. The wave function density-phase plots in Fig. 4(a) show that the density modulation in the two

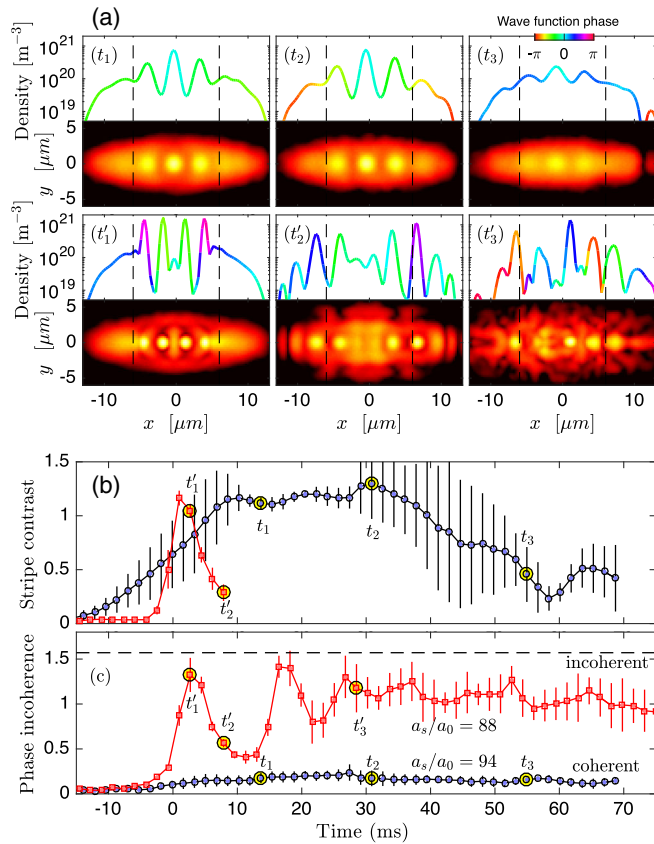


FIG. 4. Simulations of stripe formation and evolution. (a) Snapshots for a simulation with coherent stripes after a ramp to $a_s/a_0 = 94$ are shown at times $(t_1, t_2, t_3) = (13.7, 30.9, 55)$ ms, while the incoherent regime can be seen in another simulation after a ramp to $a_s/a_0 = 88$ for $(t'_1, t'_2, t'_3) = (2.7, 7.9, 28.5)$ ms. Density cuts $n(x, 0, 0)$ —with color representing the wave function phase—and column densities $\int dz n(x, y, z)$ are shown. (b) Stripe contrast \mathcal{C} for stable stripes with $a_s/a_0 = 94$ (blue circles) and unstable stripes with $a_s/a_0 = 88$ (red squares). The error bars represent standard deviations for six simulations, each with different initial noise. (c) Phase incoherence, $\alpha^l = \int^\tau dx dy n |\alpha - \langle \alpha \rangle| / \int^\tau dx dy n$, where $\alpha(x, y, 0)$ is the wave function phase, $\langle \alpha \rangle$ is its average over τ , defined as the region between the dashed lines in (a) [32]. The limit $\alpha^l = 0$ indicates global phase coherence, while $\alpha^l = \pi/2$ signals incoherence.

regimes has a different nature. In the stripe regime [Fig. 4(a), top panels], the modulation originates from the formation of an array of weakly bound droplets along the x direction, on top of a sizable BEC background that provides a coherent link between the droplets; the modulation slowly decays in time due to three-body losses, and eventually a moderately excited BEC is recovered at long times. The phase α of the wave function remains approximately uniform during the whole time evolution, apart from a small parabolic phase profile that corresponds to an axial breathing mode excited by the changing density distribution at the initial instability. The modulation has a characteristic momentum of $k_x = 1.6 \mu\text{m}^{-1}$, in agreement with the analytics [11], and hence larger than the experimentally measured values. We attribute such a difference to non-negligible interactions effects during the expansion dynamics [39]. In the incoherent regime, in the absence of three-body losses, our numerics predicts the formation of an array of tightly bound droplets [32]. In contrast to the stripe regime, they would present no significant overlap and they would tend to repel the BEC background [see, e.g., Fig. 4(a), bottom left], and hence they would rapidly become incoherent [26]. However, in the presence of experimental losses [Fig. 4(a), bottom panels], although tightly bound droplets develop initially, the larger peak density causes their very rapid decay before they can reach an equilibrium situation. The droplet decay results in strong excitations that cause violent density fluctuations in both the x and y directions. These density fluctuations result in the irregular, incoherent patterns that we observe experimentally after the free expansion.

We have numerically studied the growth of the density modulation as well as the phase profile, averaging over different realizations (characterized by different initial fluctuations). For the stripe regime, the calculated stripe contrast \mathcal{C} in Fig. 4(b)—defined as the amplitude of the stripe density oscillations divided by the amplitude of an overall Thomas-Fermi fit [32]—is in good agreement with the experimental observable A [Fig. 2(b)]. An initial growth over approximately 10 ms is followed by a plateau for 30 ms, and a later decay towards zero. The apparent longer growth time in the simulations arises because the momentum space observable A at the beginning of the pattern growth depends quadratically on the position space quantity \mathcal{C} . Figure 4(c) shows the phase incoherence α^l (defined in the caption of Fig. 4) after removing the parabolic phase profile due to the breathing oscillation [32]. Remarkably, the spatial variation of the phase remains very small during the whole evolution, indicating the presence of a robust phase locking of the stripes. The numerically observed formation of coherent stripes is in agreement with the small $\Delta\phi^2$ of Fig. 3(a). In contrast, the phase variation is very large in the incoherent regime (the observed modulation in α^l is given by the nucleation and unraveling of unstable droplets). Note that, since the interference phase is sensitive

to both wave function phase and stripe stability, we accordingly observe strong fluctuations of ϕ [Fig. 3(a)] when C fluctuates [Fig. 4(b)], although α is still coherent. We attribute the contrast fluctuations around 30–50 ms, when A is still large, to an effect of three-body losses.

The novel stripe regime hence reveals supersolid properties due to the coexistence of phase coherence and density modulation. In the absence of losses, our numerics reveals the formation of stable coherent stripes, which would still be in an excited state as a result of crossing the first-order phase transition when ramping down the scattering length [32]. However, three-body losses render the stripe pattern eventually unstable in our experiments, with a lifetime of approximately 30 ms. This instability is, however, not related to the loss of phase coherence since the latter remains high at any time despite quantum and thermal phase fluctuations, three-body losses, and the breathing oscillation [Fig. 4(c)]. Our analysis shows that the finite lifetime of coherent stripes rather results from the eventual instability of the stripe modulation [Fig. 4(b)], which leads to the experimentally observed time dependence of both A and $\Delta\phi^2$. Once the density modulation vanishes, the system remains highly coherent, in agreement with our experimental observation at long times of a large BEC, in stark contrast to our observation in the incoherent regime [Fig. 1(a)] [32].

In summary, we report in this Letter on a novel regime in a dipolar quantum gas, formed by overlapping weakly bound droplets, that exists in a narrow range of scattering lengths close to the roton instability. Because of its simultaneous phase coherence and density modulation, this regime exhibits the properties of an excited, metastable supersolid. Whereas the excitation occurs in any case due to the crossing of a first-order phase transition, the observed metastability stems from three-body losses, which in our case limit the lifetime to approximately 30 ms. Longer lifetimes might be achieved by searching magnetic-field regions in Dy isotopes with lower loss rates, or going to larger scattering lengths using larger atom number and less confining traps. Longer lifetimes will be important to test the stripe superfluidity, which is a prerequisite to assess their supersolid nature [1–4].

We acknowledge funding by the EC-H2020 research and innovation program (Grant No. 641122—QUIC) and the DFG (SFB 1227 DQ-mat and FOR 2247). R. N. B. was supported by the European Union’s Horizon 2020 research and innovation program under Marie Skłodowska-Curie Grant Agreement No. 793504 (DDQF). We acknowledge support by L. A. Gizzi, S. Gozzini, and M. Inguscio, useful conversations with M. Fattori, G. Ferrari, and S. Stringari, and technical assistance from A. Barbini, F. Pardini, M. Tagliaferri, and M. Voliani.

Note added.—We recently became aware of a complementary theoretical and experimental investigation [40], which

was motivated by our initial observations. The new theoretical analysis of this revised version confirms and complements their numerical results. Even more recently, experiments on different atomic species have shown similar phenomena, with longer lifetimes [41].

*Corresponding author.
modugno@lens.unifi.it

- [1] A. F. Andreev and I. M. Lifshitz, *Sov. Phys. JETP* **29**, 1107 (1969).
- [2] A. J. Leggett, *Phys. Rev. Lett.* **25**, 1543 (1970).
- [3] G. V. Chester, *Phys. Rev. A* **2**, 256 (1970).
- [4] M. Boninsegni and N. V. Prokof'ev, *Rev. Mod. Phys.* **84**, 759 (2012).
- [5] D. Y. Kim and M. H. W. Chan, *Phys. Rev. Lett.* **109**, 155301 (2012).
- [6] J. Léonard, A. Morales, P. Zpancic, T. Esslinger, and T. Donner, *Nature (London)* **543**, 87 (2017).
- [7] J. R. Li, J. Lee, W. Huang, S. Burchersky, B. Shteynas, F. Ç. Topi, A. O. Jamison, and W. Ketterle, *Nature (London)* **543**, 91 (2017).
- [8] T. Lahaye, C. Menotti, L. Santos, M. Lewenstein, and T. Pfau, *Rep. Prog. Phys.* **72**, 126401 (2009).
- [9] M. A. Baranov, M. Dalmonte, G. Pupillo, and P. Zoller, *Chem. Rev.* **112**, 5012 (2012).
- [10] L. Santos, G. V. Shlyapnikov, and M. Lewenstein, *Phys. Rev. Lett.* **90**, 250403 (2003).
- [11] L. Chomaz, R. M. W. van Bijnen, D. Petter, G. Faraoni, S. Baier, J. H. Becher, M. J. Mark, F. Wächtler, L. Santos, and F. Ferlaino, *Nat. Phys.* **14**, 442 (2018).
- [12] D. Petter, G. Natale, R. M. W. van Bijnen, A. Patscheider, M. J. Mark, L. Chomaz, and F. Ferlaino, [arXiv:1811.12115](https://arxiv.org/abs/1811.12115).
- [13] S. Komineas and N. R. Cooper, *Phys. Rev. A* **75**, 023623 (2007).
- [14] A. Macia, D. Hufnagl, F. Mazzanti, J. Boronat, and R. E. Zillich, *Phys. Rev. Lett.* **109**, 235307 (2012).
- [15] Z.-K. Lu, Y. Li, D. S. Petrov, and G. V. Shlyapnikov, *Phys. Rev. Lett.* **115**, 075303 (2015).
- [16] F. Cinti and M. Boninsegni, *Phys. Rev. A* **96**, 013627 (2017).
- [17] D. S. Petrov, *Phys. Rev. Lett.* **115**, 155302 (2015).
- [18] F. Wächtler and L. Santos, *Phys. Rev. A* **93**, 061603(R) (2016).
- [19] H. Saito, *J. Phys. Soc. Jpn.* **85**, 053001 (2016).
- [20] D. Baillie, R. M. Wilson, R. N. Bisset, and P. B. Blakie, *Phys. Rev. A* **94**, 021602(R) (2016).
- [21] R. N. Bisset, R. M. Wilson, D. Baillie, and P. B. Blakie, *Phys. Rev. A* **94**, 033619 (2016).
- [22] H. Kadau, M. Schmitt, M. Wenzel, C. Wink, T. Maier, I. Ferrier-Barbut, and T. Pfau, *Nature (London)* **530**, 194 (2016).
- [23] I. Ferrier-Barbut, H. Kadau, M. Schmitt, M. Wenzel, and T. Pfau, *Phys. Rev. Lett.* **116**, 215301 (2016).
- [24] L. Chomaz, S. Baier, D. Petter, M. J. Mark, F. Wächtler, L. Santos, and F. Ferlaino, *Phys. Rev. X* **6**, 041039 (2016).
- [25] M. Schmitt, M. Wenzel, B. Böttcher, I. Ferrier-Barbut, and T. Pfau, *Nature (London)* **539**, 259 (2016).
- [26] M. Wenzel, F. Böttcher, T. Langen, I. Ferrier-Barbut, and T. Pfau, *Phys. Rev. A* **96**, 053630 (2017).

- [27] D. Baillie and P. B. Blakie, *Phys. Rev. Lett.* **121**, 195301 (2018).
- [28] S. M. Rocuzzo and F. Ancilotto, [arXiv:1810.12229](https://arxiv.org/abs/1810.12229).
- [29] E. Lucioni, G. Masella, A. Fregosi, C. Gabbanini, S. Gozzini, A. Fioretti, L. Del Bino, J. Catani, G. Modugno, and M. Inguscio, *Eur. Phys. J. Spec. Top.* **226**, 2775 (2017).
- [30] E. Lucioni, L. Tanzi, A. Fregosi, J. Catani, S. Gozzini, M. Inguscio, A. Fioretti, C. Gabbanini, and G. Modugno, *Phys. Rev. A* **97**, 060701(R) (2018).
- [31] Y. Tang, A. G. Sykes, N. Q. Burdick, J. M. DiSciaccia, D. S. Petrov, and B. L. Lev, *Phys. Rev. Lett.* **117**, 155301 (2016).
- [32] See Supplemental Material at <http://link.aps.org/supplemental/10.1103/PhysRevLett.122.130405>, which includes Refs. [33–38], for more information on the experimental and theoretical methods.
- [33] S. Roy, M. Landini, A. Trenkwalder, G. Semeghini, G. Spagnolli, A. Simoni, M. Fattori, M. Inguscio, and G. Modugno, *Phys. Rev. Lett.* **111**, 053202 (2013).
- [34] S. Giovanazzi, P. Pedri, L. Santos, A. Griesmaier, M. Fattori, T. Koch, J. Stuhler, and T. Pfau, *Phys. Rev. A* **74**, 013621 (2006).
- [35] A. R. P. Lima and A. Pelster, *Phys. Rev. A* **86**, 063609 (2012).
- [36] A. R. P. Lima and A. Pelster, *Phys. Rev. A* **84**, 041604(R) (2011).
- [37] S. Ronen, D. C. E. Bortolotti, and J. L. Bohn, *Phys. Rev. A* **74**, 013623 (2006).
- [38] P. B. Blakie, A. S. Bradley, M. J. Davis, R. J. Ballagh, and C. W. Gardiner, *Adv. Phys.* **57**, 363 (2008).
- [39] J. Billy, E. A. L. Henn, S. Müller, T. Maier, H. Kadau, A. Griesmaier, M. Jona-Lasinio, L. Santos, and T. Pfau, *Phys. Rev. A* **86**, 051603(R) (2012).
- [40] F. Böttcher, J.-N. Schmidt, M. Wenzel, J. Hertkorn, M. Guo, T. Langen, and T. Pfau, [arXiv:1901.07982](https://arxiv.org/abs/1901.07982) [*Phys. Rev. X* (to be published)].
- [41] L. Chomaz *et al.*, [arXiv:1903.04375](https://arxiv.org/abs/1903.04375).